BLUE-ORANGE EMISSION FROM Sm^{3+} ACTIVATED $LaCePO_4$ PHOSPHOR FOR DISPLAY APPLICATIONS

K. Lakshmi [1], M. C. Rao [1,2*], K. V. R. Murthy [3], Vikas Dubey [4]

[1] Department of Physics, Krishna University, Machilipatnam, India; e-mail: raomc72@gmail.com
[2] Department of Physics, Andhra Loyola College, Vijayawada, India
[3] Department of Applied Physics, Faculty of Engineering and Technology, M.S. University of Baroda, Vadodara, India
[4] Department of Physics, North-Eastern Hill University (NEHU), Shillong, Meghalaya, India

We discuss new features of Sm^{3+} doped $LaCePO_4$ phosphor as a potential candidate for display applications. Mainly, the traditional modified solid-state synthesis technique was used to prepare the samples. The X-ray diffraction technique was used for the structural studies. $LaCePO_4:Sm^{3+}$ phosphor production was verified by Fourier transform infrared studies. It was customary to use scanning electron microscopy to learn more about the morphology of the prepared samples. Additionally, photoluminescence (PL) analysis of the phosphor samples was presented for different doping ion concentrations with various excitations. In the presence of Sm^{3+}, $LaCePO_4$ emits powerful blue and orange emissions. In-depth research was carried out on the transitions between the concentration quenching effect and the doping ion. The distribution of the spectral region estimated from PL emission spectra was shown in the 1931 Commission International de l'Éclairage (x,y) chromaticity coordinates and was located (0.20,0.22) in the blue region. According to our research, as-prepared phosphor may find useful application in display devices, especially because of its blue and orange content.

Keywords: *phosphor, UV converted LED, CIE coordinates, photoluminescence.*

СИНЕ-ОРАНЖЕВОЕ ИЗЛУЧЕНИЕ АКТИВИРОВАННОГО ИОНАМИ Sm^{3+} ЛЮМИНОФОРА $LaCePO_4$ ДЛЯ ДИСПЛЕЕВ

K. Lakshmi [1], M. C. Rao [1,2*], K. V. R. Murthy [3], V. Dubey [4]

УДК 535.37

[1] Университет Кришны, Мачилипатнам, Индия; e-mail: raomc72@gmail.com
[2] Колледж Андхра Лойола, Виджаявада, Индия
[3] Университет Бароды, Вадодара, Индия
[4] Северо-Восточный Университет (NEHU), Шиллонг, Мегхалая, Индия

(Поступила 22 ноября 2022)

Рассмотрены особенности люминофора $LaCePO_4$, легированного Sm^{3+}, для применения в дисплеях. Образцы, изготовленные традиционным модифицированным методом твердотельного синтеза, исследованы методами рентгеновской дифракции и ИК-Фурье-спектроскопии. Для более подробного изучения морфологии приготовленных образцов использована сканирующая электронная микроскопия. Представлен анализ фотолюминесценции (ФЛ) образцов люминофоров для разных концентраций легирующих ионов с возбуждением различных длин волн. В присутствии Sm^{3+} $LaCePO_4$ излучает мощное синее и оранжевое свечение. Распределение спектральной области, оцененное по спектрам ФЛ, в координатах цветности Международной комиссии по освещению (x,y) 1931 г. располагается (0.20,0.22) в синей области. Полученный люминофор может найти применение в устройствах отображения.

Ключевые слова: *люминофор, УФ-преобразованный светодиод, координаты CIE, фотолюминесценция.*

Introduction. Commercial phosphors often require low-cost and effective performance in lamp applications as prerequisites. By selecting the right host lattices, costs can be reduced, specifically by selecting host lattices that can be manufactured at lower temperatures and that do not demand pricey raw ingredients. Numerous factors affect how well and how efficiently phosphors work when used in lamps [1]. By contrasting the luminous characteristics of new phosphors with those of the industry standard phosphors, investigating the performance of new phosphors on a laboratory scale is required. The green-emitting $CeMgAl_{11}O_{19}:Tb^{3+}$, $GdCeMgB_5O_{10}:Tb^{3+}$, and $LaCePO_4:Tb^{3+}$ are the recognized commercial standard materials [2]. When compared with the other RE^{3+} ions, it is more interesting to study the fluorescence properties of the materials doped with Sm^{3+} ions, because of their practical significance in the fields of color displays, solid-state lasers, high-density memory devices, and underwater communications, among others [3, 4]. In the visible area, Sm^{3+} ions exhibit four distinct emission bands that correspond to ${}^4G_{5/2}$, ${}^6H_{5/2}$, ${}^6H_{7/2}$, ${}^6H_{9/2}$, and ${}^6H_{11/2}$ transitions. The phonon energy of the borate glasses (1300–1600 cm^{-1}) is significantly lower than the energy gap (7000 cm^{-1}) between the ${}^4G_{5/2}$ emission level and the next lower level of Sm^{3+} ions [3], which results in a negligible multi-phonon nonradiative decay in the case of Sm^{3+} ions. As a result, emissions corresponding to the ${}^4G_{5/2}$ level of the Sm^{3+} ions also exhibit higher quantum efficiency.

A physical, structural, and spectroscopic study on Sm^{3+} doped ZnO mixed alkali borate glass was published by Sailaja et al. [5]. Krause et al. [6] explored the functioning of the network modifier PbO in Sm^{3+} doped borate glass. By using a solid-state reaction approach, Nagaraja et al. [7] investigated the optical and luminescent characteristics of Sm^{3+} ion-doped $NaCaAlPO_4F_3$ phosphor. The impact of Sm^{3+} ion concentration on the structure and luminescent characteristics of lithium borate glass has been studied by Ramteke et al. [8]. Sd. Ahamed et al. [9] investigated the spectroscopic and laser characteristics of lithium fluoroborate glass doped with Sm^{3+} ions. The photoluminescence studies of various Sm^{3+} ion concentrations and the impact of various excitations have been reported in this publication. A modified solid-state reaction technique was used to produce Sm^{3+} ion-doped $LaCePO_4$ phosphor. By using X-ray diffraction (XRD) and scanning electron microscopy (SEM), the structure and morphology of the as-prepared phosphor were analyzed. By examining the color coordinates and color ratios of Sm^{3+} ion-doped $LaCePO_4$ phosphor, the bright color was identified. The chromaticity coordinate values were determined using Commission Internationale de l'Éclairage (CIE) 1931 data of the Sm^{3+} ion-doped $LaCePO_4$ phosphor.

Experimental. Variable concentrations (x = 0.5, 1.0, 1.5, and 2.0 mol.%) of Sm^{3+}-doped $LaCePO_4$ phosphors were prepared via solid-state synthesis. High-purity La_2O_3, $NH_4H_2PO_4$, CeO_2, and Sm_2O_3 were generally used as starting ingredients without any additional purification. All of the original ingredients were first weighed and blended together in the correct ratios. These combined powders were then placed in an alumina crucible for calcination at 500°C for 2 h and after cooling, samples were taken for further sintering in the air at 900°C for 2 h.

The XRD patterns of the samples were recorded with a Bruker AXS D8 Advance, which primarily worked with the Bragg–Brentano focusing geometry. As a primary X-ray source, CuK_α radiation (λ = 1.54060 Å) was used. These instruments were typically run at a minimal operating current of 30.00 mA and a high voltage of 40 kV. With a scan rate of roughly 5°/min within the 10–80° range, the XRD patterns were seen. Perkin Elmer Spectrum 100 Fourier transform infrared (FTIR) spectrometer measures different bands within the produced phosphor and analyzes functional groups, if any, as well as the bending and stretching of bonds in the fingerprint region. The morphology of these samples was examined using a JEOL JSM-6390LV scanning electron microscope. Under UV-visible excitation, the spectrofluorophotometer instruments (RF-5301PC Shimadzu) were used to capture the excitation spectra and photoluminescence (PL) emission of the samples. Using the LUMPAC program, the emission spectra of the phosphor samples were used to determine the CIE chromaticity coordinates [10–12].

Results and discussion. The XRD patterns of the $LaCePO_4:Sm^{3+}$ (1.0 mol.%) sample are displayed in Fig. 1. Nearly a single phase with some impurities is visible in the XRD pattern. The width of the peak expands as the particle size is decreased. Using Scherrer's formula [13–20], the size D of the particles was calculated from the full-width half-maximum (FWHM) of each peak

$$D = 0.9\lambda/(\beta\cos\theta), \quad (1)$$

where λ is the X-ray wavelength, β is the FWHM, and θ is the diffraction angle. The average crystallite size of the prepared phosphor was found to be 78.26 nm.

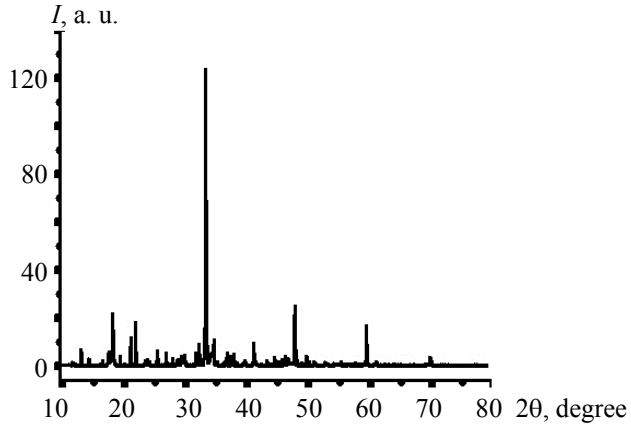

Fig. 1. XRD patterns of 1.0 mol.% Sm^{3+}-doped $LaCePO_4$ phosphor.

The FTIR spectrum of the $LaCePO_4$:Sm^{3+} (1.0 mol.%) phosphor (Fig. 2) shows that it has more peaks in the fingerprint area than the control sample. This may be a result of vibrations caused by the metal-ligand stretching or bending. According to the literature, no researchers have provided the FTIR spectrum of this phosphor. La–O vibrations are shown by the peak centering at 990 cm^{-1}, Ce–O vibrations are shown by the peak centering at 1001 cm^{-1}, and Sm–O vibrations are shown by the higher side peak centering at 1630 cm^{-1}, confirming the creation of $LaCePO_4$:Sm^{3+} phosphor [21, 22].

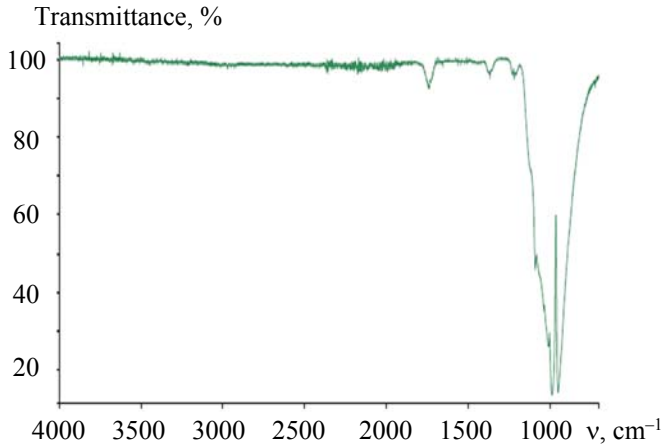

Fig. 2. FTIR spectrum of 1.0 mol.% Sm^{3+}-doped $LaCePO_4$ phosphor.

The SEM micrographs of 1.0 mol.% Sm^{3+}-doped samples are displayed in Fig. 3 at various magnifications. The particle size ranges from a few micrometers to a few nanometers and the micrographs clearly show that the particles crystallized in an inhomogeneous morphology that exhibits grain growth tendency and agglomeration when prepared at high temperatures. This gradient in particle size is expected as these samples are known to agglomerate and need specific, long ball milling to form homogeneous morphology.

The excitation spectrum of $LaCePO_4$:Sm^{3+} (1.0 mol.%) phosphor, which is monitored at 598 nm, is shown in Fig. 4a. The excitation of an electron from the oxygen 2*p* state to a Sm^{3+} 4*f* state is known to be the cause of the band near 277 nm, which is associated with a charge transfer process. The well-known $^4G_{5/2}\rightarrow{}^6H_J$ (J = 5/2, 7/2) line emissions of the Sm^{3+} ions were shown accurately in emission spectra with 277 nm UV excitation radiation. According to the findings in Fig. 4b, the spectral profiles of the phosphors shift significantly with changing Sm^{3+} ion concentrations. The plots demonstrate that after 1.0 mol.%, the emission intensity for all phosphors reaches its maximum luminescence intensity and there after falls with increasing concentration. The peak position of the emission spectra is unaffected by rising Sm^{3+} ion concentrations. At 1.0 mol.% of Sm^{3+} ions, the concentration quenches (Fig. 4b). This concentration quenching was caused by a typical cross-relaxation interaction, which eventually reduces the intensity of the emission.

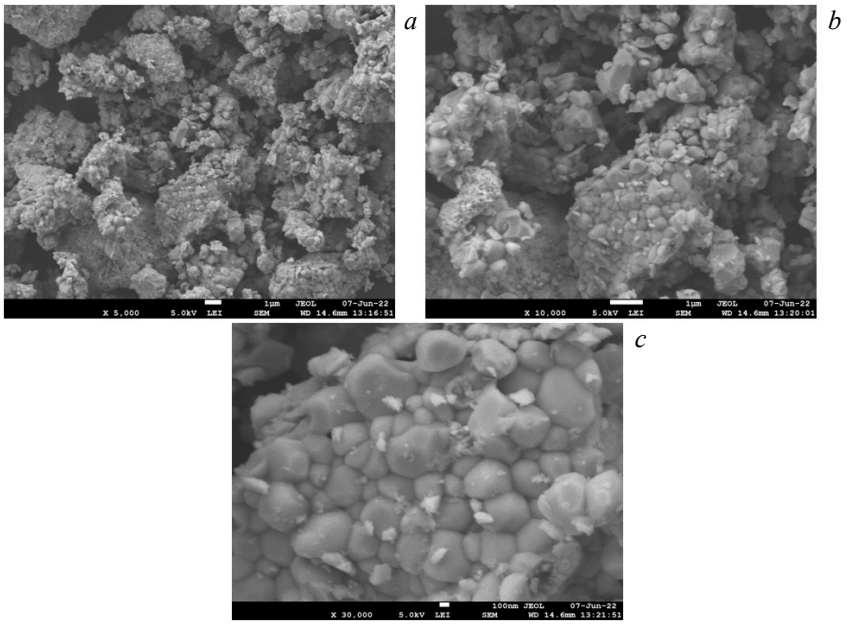

Fig. 3. SEM images of 1.0 mol.% Sm^{3+}-doped $LaCePO_4$ phosphor with different magnifications.

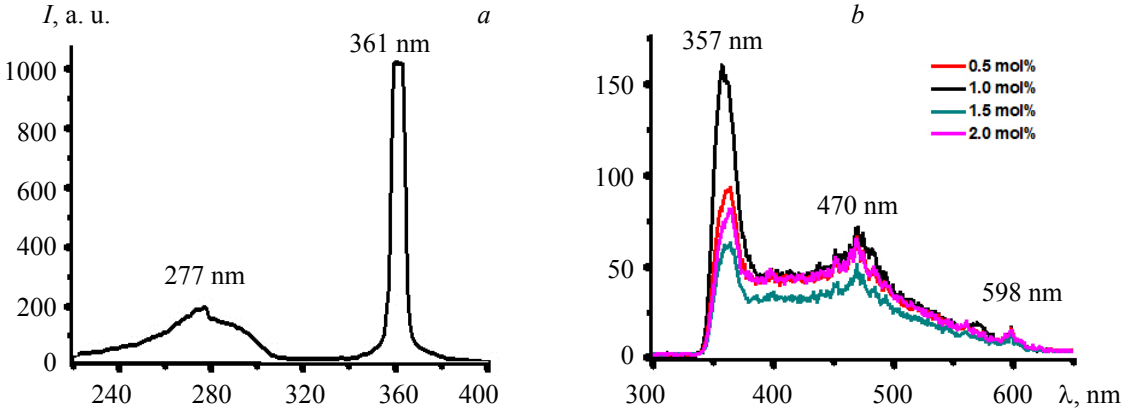

Fig. 4. PL excitation spectrum of $LaCePO_4$:Sm^{3+} (1.0 mol.%) phosphor (a) and PL emission spectra of $LaCePO_4$:Sm^{3+} phosphor with different concentrations (b).

The identified emission bands were due to the intra-4*f* transitions of Sm^{3+} ions. Among these, the transition has the strongest intensity and this can be applied to the yellow-orange emitting display materials. A second intense peak at 598 nm is due to transition and this can be applied to the blue-orange emission. Magnetic dipole transitions obey the selection rule of $\Delta J = 0$ and ± 1 and electric dipole transitions obey the selection rule of $\Delta J \leq 6$ unless J or $J' = 0$, when $\Delta J = 2, 3, 6$ [11, 12]. These intra-4*f* transitions of Sm^{3+} ions, such as $^4I_{13/2} \rightarrow {}^6H_{5/2}$ at 470 nm [23] and $^4G_{5/2} \rightarrow {}^6H_{7/2}$ at 598 nm, were responsible for the detected emission bands. The strongest intensity of these transitions can be applied to the yellow-orange-emitting display materials, specifically the transition $^6H_{5/2} \rightarrow {}^4I_{11/2}$. The $^4G_{5/2} \rightarrow {}^6H_{7/2}$ transition causes a second intense peak at 598 nm, which can be applied to the blue-orange emission.

Malashkevich et al. [24] reported that samarium centers into silica gel glass sintered at 1250°C in the triply charged state. By far the greater fractions of its ions form optical centers of one type. Such centers are characterized by the weak cross-relaxation interaction of Sm^{3+} ions and a sizable fraction of photons (45%) emitted in the ultrasensitive electric dipole transition $^4G_{5/2} \rightarrow {}^6H_{7/2}$. The co-activation of Sm-containing glasses with cerium results in the formation of a new type of optical center in the pore nucleation stage. The Sm^{3+} ions in these complex centers are characterized on average by higher local symmetry and efficient enhance-

ment of luminescence by photoreduced cerium ions. The cross-relaxation interactions of Sm^{3+} ions in the subsystem of these centers are weak, but the extinction of their luminescence is comparatively efficient. In our study, the peak centered at 357 nm in the near UV region and broadband at 470 nm indicated transitions from the ground-state $^6H_{5/2}$ of Sm^{3+} ions to higher energy states [25].

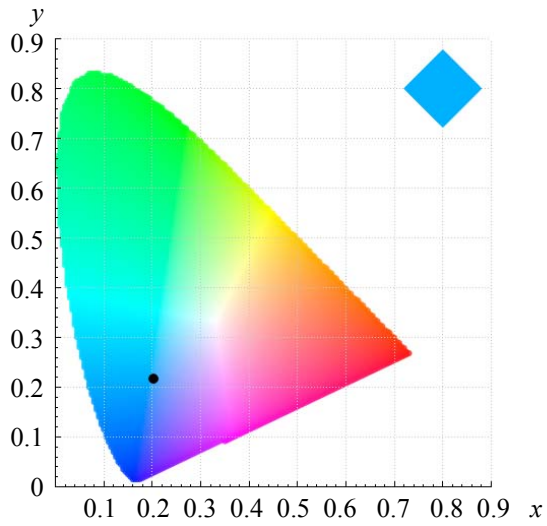

Fig. 5. CIE 1931 coordinates of $LaCePO_4:Sm^{3+}$ (1.0 mol.%) phosphor ($x = 0.20$, $y = 0.22$).

The findings suggest that $LaCePO_4:Sm^{3+}$ (1.0 mol.%) phosphors might be chosen as suitable candidates for application in display devices (λ_{ex} = 277 nm). However, the fundamental color balance for blue-orange light emission is determined by the relative intensities of the emission bands. This was accomplished for the 1.0 mol.% sample with the spectrum shown in Fig. 5 because it brought the CIE 1931 chromaticity coordinates much closer to the blue light. Examining the fluorescence light spectral profile as a function of activator concentration revealed that, for different activator concentrations, the chromaticity coordinates of the overall emission light altered, resulting in distinct hues of overall emission light [12, 26–31].

Conclusions. The solid-state reaction technique was used to prepare $LaCePO_4$ phosphor that had been doped with various concentrations of Sm^{3+} ions. The production of a single phase was confirmed by the XRD examination and it was discovered that the average crystallite size of the produced phosphor was 78.26 nm. LaCePO4:Sm^{3+} phosphor production was verified by FTIR. The SEM micrographs showed a sphere-like structure with particles ranging in size from a few microns to a few nanometers. After being excited in the ultraviolet region, photoluminescence emission studies revealed the distinctive emission lines of Sm^{3+} ions between 350 and 650 nm as a result of their intra-center transitions. The charge transfer bands that exist in the excitation spectra have been thoroughly described. At a certain point, the increase in Sm^{3+} concentration reduced the PL intensity; however, above that point, the PL intensity dropped owing to concentration quenching. The distribution of the spectral region was shown in the 1931 CIE (x,y) chromaticity coordinates and it was located (0.20,0.22) in the blue region. This finding suggests that the produced phosphor is an effective emitter for UV light excitations.

REFERENCES

1. T. Justel, H. Nikol, C. Ronda, *Angew. Chem., Int. Ed.*, **37**, 3084–3103 (1998).
2. G. Blasse, E. C. Grabmaier, *Luminescent Materials*, Springer-Verlag, Berlin (1994).
3. P. V. Do, V. P. Tuyen, V. X. Quang, L. X. Hung, L. D. Thanh, T. Ngoc, N. V. Tam, B. T. Huy, *Opt. Mater.*, **55**, 62–67 (2016).
4. F. Wang, B. J. Chen, H. Lin, E. Y. B. Pun, *J. Quant. Spectrosc. Radiat. Transfer*, **147**, 63–70 (2014).
5. B. Sailaja, R. Joyce Stella, G. Thirumala Rao, B. Jaya Raja, V. Pushpa Manjari, R. V. S. S. N. Ravikumar, *J. Mol. Struct.*, **1096**, 129–135 (2015).
6. S. Krause, C. Pfau, M. Dyrba, P. T. Miclea, S. Schweizer, *J. Lumin.*, **151**, 29–33 (2014).

7. R. Nagaraja, V. Pushpa Manjari, B. Sailaja, R. V. S. S. N. Ravikumar, *J. Mol. Struct*., **1130**, 96–102 (2017).
8. D. D. Ramteke, V. Y. Ganvira, S. R. Munishwara, R. S. Gedam, *Phys. Proc*., **76**, 25–30 (2015).
9. Sd. Z. A. Ahamed, C. M. Reddy, B. D. P. Raju, *Spectrochim. Acta*, **103**, 246–254 (2013).
10. Y. Li, Y. Xia, S. Liao, Q. Long, X. Zhao, S. Dai, K. Lu, *Mater. Lett*., **123**, 112–115 (2014).
11. V. Dubey, J. Kaur, S. Agrawal, N. S. Suryanarayana, K. V. R. Murthy, *Superlattices Microstruct*., **67**, 156–171 (2014).
12. J. Kaur, D. Singh, N. S. Suryanarayana, V. Dubey, *J. Display Tech*., **12**, No. 9, 928–932 (2016).
13. G. Phaomei, W. R. Singh, R. S. Ningthoujam, *J. Lumin*., **131**, No. 6, 1164–1171 (2011).
14. G. Li, L. Li, M. Li, Y. Song, H. Zou, L. Zou, S. Gan, *Mater. Chem. Phys*., **133**, No. 1, 263–268 (2012).
15. C. R. Kesavulu, C. Basavapoornima, C. D. Viswanath, C. K. Jayasankar, *J. Lumin*., **171**, 51–57 (2016).
16. Y. Xia, Y. Huang, Q. Long, S. Liao, Y. Gao, J. Liang, J. Cai, *Ceram. Int*., **41**, No. 4, 5525–5530 (2015).
17. X. Wang, X. Zheng, L. Zhang, *J. Alloys Compd*., **632**, 269–273 (2015).
18. M. C. Rao, *J. Optoelect. Adv. Mater*., **13**, No. 1-2, 78–81 (2011).
19. K. Ravindranadh, B. Babu, C. V. Reddy, J. Shim, M. C. Rao, R. V. S. S. N. Ravikumar, *Appl. Mag. Res*., **46**, No. 1, 1–15 (2015).
20. Sk. Muntaz Begum, G. Nirmala, K. Ravindranadh, T. Aswani, M. C. Rao, *J. Mol. Struct*., **1006**, No. 1, 344–347 (2011).
21. I. Kumar, A. K. Gathania, *J. Mater. Sci.: Mater. Electron*., **33**, No. 1, 328–341 (2022).
22. G. Bekiaris, C. Peltre, L. S. Jensen, S. Bruun, *Spectrochim. Acta A: Mol. Biomol. Spectrosc*., **168**, 29–36 (2016).
23. Y. A. Tanko, M. R. Sahar, S. K. Ghoshal, *Results Phys*., **6**, 7–11 (2016).
24. G. E. Malashkevich, I. M. Mel'nichenko, E. N. Poddenezhnyi, A. V. Semchenko, *Phys. Solid State*, **40**, 420–426 (1998).
25. V. Singh, A. Yadav, C. B. A. Devi, A. S. Rao, N. Singh, *Optik*, **242**, 167264 (2021).
26. J. Zou, Q. Zhu, J. G. Li, *Cryst. Eng. Commun*., **22**, No. 25, 4289–4300 (2020).
27. T. Gavrilović, J. Periša, J. Papan, K. Vuković, K. Smits, D. J. Jovanović, M. D. Dramićanin, *J. Lumin*., **195**, 420–429 (2018).
28. T. Lyu, P. Dorenbos, *J. Mater. Chem. C*, **6**, No. 2, 369–379 (2018).
29. B. Lei, S. Q. Man, Y. Liu, S. Yue, *Mater. Chem. Phys*., **124**, No. 2-3, 912–915 (2010).
30. Z. Ju, R. Wei, J. Zheng, X. Gao, S. Zhang, W. Liu, *Appl. Phys. Lett*., **98**, No. 12, 121906 (2011).
31. R. B. Basavaraj, H. Nagabhushana, B. D. Prasad, S. C. Sharma, S. C. Prashantha, B. M. Nagabhushana, *Optik*, **126**, No. 19, 1745–1756 (2015).